Research Article

Introducing SNAP: a novel pedal-assisted electric ultralight vehicle

Francesco Passarella[1,2] · Giacomo Mantriota[2] · Giulio Reina[2]

Received: 28 July 2022 / Accepted: 14 December 2022

Published online: 25 December 2022

Abstract
Innovation in transportation and mobility is central to sustainable development. There is a widespread awareness that society would benefit if transportation became more sustainable, promoting economic growth while respecting the environment. This paper introduces SNAP, a four-wheel pedal-assisted electric vehicle that represents a new concept in sustainable mobility towards filling the gap between bicycle and automobile. The choice of the architecture for the hybrid powertrain where the driver pedals are assisted with an electric motor is discussed along with the experimental analysis of the power loss associated with the single components of the transmission. In turn, this knowledge allows the overall quadricycle performance to be evaluated in terms of maximum speed, efficiency, and travel range at varying operating conditions that include vehicle load, road slope, and gear change. It is shown that SNAP can be a promising answer to address the problem of sustainable and safe micro mobility of persons and goods in urban settings.

Highlights

- A novel concept of pedal-assisted quadricycle for sustainable and safe urbanmicro mobility of persons and goods
- Analysis of the hybrid powertrain transmission that combines the driver pedalswith an assisting electric motor
- Performance evaluation in terms of maximum speed, efficiency, and travel rangeat varying operating conditions

Keywords SDG7 · SDG11 · Electric-assisted vehicles · Quadricycle · Pedelec · Mobility · Last-mile delivery · Powertrain design · Transmission power loss · Electric vehicle efficiency

1 Introduction

One of the main objectives of scientific research in the automotive sector is the reduction of CO2 emissions. Because of this effort towards greener propulsion, powertrain architectures have changed massively in the last decades. The current scenario of electrified mobility is dominated by high or mid-power automobiles designed to provide adequate performance in a wide range of driving conditions (urban, non-urban, highways, etc.). These architectures feature:

- powerful (and therefore bulky) battery packs that contribute significantly to vehicle mass and cost. Addition-

✉ Giulio Reina, giulio.reina@poliba.it | [1]SNAP s.r.l., 72100 Bari, Italy. [2]Department of Mechanics, Mathematics and Management, Politecnico Di Bari, Via Orabona 4, 70126 Bari, Italy.

ally, production and disposal of batteries generate high carbon emissions. According to recent works on the subject [1] the production of lithium batteries releases 75 kgCO2/kWh in the atmosphere. For example, the production of a 45 kWh battery, suitable for a mid-power electric vehicle, generates the same amount of CO2 of an internal combustion engine car that drives for 30,000 km;

- large vehicle mass that causes high electric energy consumption, especially in urban environments, with consequent CO2 emissions caused by the fact that electric energy is currently mainly obtained from fossil fuels.

Recent studies even claim that electric vehicles might have a larger carbon footprint than gasoline cars homologated to the most recent standards [2].

It is important to consider that the complete transition to renewable sources for electricity production is an ongoing process that will last for several decades to come. Furthermore, to account for the energy required if all vehicles were electric, the production of electricity should be increased by 60%. Therefore, the best short-term strategy to reduce carbon emissions is to drastically improve the energy requirements of electric vehicles.

In this context, the reduction of energy consumption can be achieved through diversification, designing each vehicle for a specific driving condition. For example, urban mobility requires low-weight, low-power vehicles with high levels of safety and comfort. In the urban driving cycle, energy consumption and emissions are directly related to the weight of the vehicle. Electric L-category Vehicles and cargo bikes (that can be assimilated to the EN15194) are lightweight and compact electric vehicles that represent a possible solution towards intelligent and green urban mobility. Indeed, ELVs and cargo bikes are the only vehicles allowed to access freely traffic-restricted areas.

On one hand, the 2020 pandemic-related recession led to a 28% contraction of car registrations (biggest reduction since 1970). On the other hand, the shared micro-mobility increased by 454% in the same period [3]. In recent years, urban mobility with e-bikes and electric scooters received a huge boost, thanks to their low weight and low power consumption. Some examples are the EE-Speed Bike [4], the Bike2 drivetrain [5], the Mando Footloose [6], the Podbike [7], the Flevobike Orca [8] and the RATH Racer [9]. Although these vehicles represent a viable solution to emissions reduction, they cannot guarantee the safety and comfort required, especially in conditions of adverse weather, heavy traffic, or lack of cycle lanes. Most of the models currently available on the market are either fairing-less or lack a comfortable driving position or easy access to the vehicle. Both conditions can be hardly found in a model and have substantially limited the widespread adoption of this type of vehicle. Additionally, despite the relatively little number of vehicles of this kind currently circulating in urban environments, new accidents are reported daily, sometimes even with fatal injuries. Moreover, e-bikes and electric scooters do not offer any room for additional loads (bags, luggage, passenger, etc.).

Therefore, Four-wheel Electric Lightweight Vehicles (FELV) represent a promising solution to the urban mobility problem, halfway between a mini-car and an e-bike. A properly designed electric lightweight vehicle could present a very low energy consumption (like an e-bike), while retaining adequate safety and comfort.

This paper presents a novel pedal-assisted electric quadricycle, named SNAP and shown in Fig. 1 that can be used for sustainable personal or goods transportation in urban environments. It complies with the EN15194 [10] as an electrically power-assisted cycle. As such, SNAP does not require any insurance coverage or plate for the EU market. It fulfills requirements of easy accessibility, high comfort and safety, and low maintenance. A closed cockpit that represents a unique feature of SNAP provides protection from adverse weather conditions. SNAP achieves a maximum speed of 25 km/h, it has a curb weight of 130 kg and a maximum payload of 160 kg, and it is powered by two 980 Wh batteries with a 60 km range (expandible to 120 km with battery swap). Two power levels are available: 250 W for the pedelec version, compliant with the EN15194, 1000 W for the speed pedelec version L1e-A. While the SNAP concept was preliminary described in [11] with the help of rendering and CAD drawings, the original contributions of this work refer to the introduction and description of the fully functioning prototype along with the exhaustive discussion of the whole power transmission and its experimental validation.

The paper is structured as follows. Section 2 describes the technical requirements in the context of the current

Fig. 1 The electric ultralight quadricycle SNAP

EU standards. A survey of existing pedal-assisted quadricycles is also presented, explaining the differences with the proposed vehicle SNAP. Section 3 focuses on the technical details of SNAP, providing an in-depth description of the hybrid powertrain transmission and the energy consumption of its single components. The overall efficiency of Snap is also evaluated during straight driving on sloped roads and at varying operating conditions. Section 4 discusses the relevance of the proposed research, whereas conclusions and lessons learnt are drawn in the final Sect. 5.

2 Current standards and design requirements

Electrically power-assisted cycles comply with the European standard EN15194 [10]. However, the SNAP refers to a special category that is not explicitly considered in this standard because it has four wheels and not two wheels. Based on EN15194 standard, cycles must limit their velocity and power, respectively, to 25 km/h and 250 W. When the power rate increases up to 1 kW, the vehicle falls in the L1e-A category, with mandatory insurance, that keeps the speed limit of 25 km/h but requires insurance coverage. Another possibility is to fall in the lightweight quadricycles, e.g., L6e category, with mandatory insurance that have a power limit of 4 kW, a maximum speed of 45 km/h, and a maximum net weight of 425 kg that is largely fulfilled by the SNAP model. Therefore, considering the existing standards, three steps of power are envisaged for the proposed vehicle to comply with all the above-mentioned categories based on the buyer requests. The vehicle chassis has been designed to withstand the worst stress conditions, e.g., approval conditions for the L6e category.

Currently, the market for this type of hybrid vehicle is not fully developed. Most of the proposed models show limited accessibility for an average user and share many components with the "velomobiles" (Fig. 2a) that are vehicles with human propulsion featuring an aerodynamic fairing and that have been adopted since the beginning of the last century. Although velomobiles are commonly used for agonistic training, they are not well suited as an urban transportation system. Another typology is that of trikes (Fig. 2b), which are less extreme than velomobiles but they are open and not waterproof. Trikes have a height from the ground that makes them not practical and dangerous in the case of impact with a car.

In addition to velomobile vehicles and trikes, there is a limited number of existing vehicles that appear to be in the same segment as SNAP. Some of the most interesting are the EAV vehicle, of the Electric Assisted Vehicles Limited (UK) company [14], the CITKAR vehicle, of the CITKAR GmbH (DE) company [15], the Armadillo vehicle, of the VELOVE (SE) company [16]. These three models are currently those with larger market coverage. They are now described in more detail. The EAV vehicle, shown on the left of Fig. 3, which is currently also used by Amazon in the UK, comes with a load volume like that of the SNAP vehicle, a chain drive system like that of the SNAP vehicle, with the difference of using a derailleur gear rather than a hub gearbox. The big difference is in the driving position; in fact, in the EAV vehicle the driver is seated on a saddle as on a normal bicycle. This driving position, compared to the configuration with a car seat, imposes a very high center of gravity on the driver, and cornering can create an unpleasant sensation as this vehicle, unlike a normal bicycle, cannot lean when cornering (no tilting).

The CITKAR vehicle [15] (Fig. 3, right side) has an excellent level of technology (drive by wire) but with a very high selling price, which starts at € 13900 excluding tax for the box version (source CITKAR official website). Inside there is a seat like in cars, but it does not have seat belts or anti-intrusion bars. The design of this vehicle is questionable from an aesthetic point of view. It has leaf spring suspensions and no there is no underbody protection of the vehicle from water and debris.

(a) (b)

Fig. 2 Examples of recumbent cycles: **a** velomobile [12], and **b** trike [13]

Fig. 3 The EAV vehicle [14] (left), and the CITKAR vehicle [15] (right)

Fig. 4 The Armadillo vehicle [16]

Finally, the Armadillo vehicle [16], shown in Fig. 4 is characterized by a traditional mechanical chain system, and does not have a bodywork, therefore users are not protected from atmospheric agents and from impacts. This vehicle also has no protection in case of rollover and does not have seat belts. The steering system is like the one present on traditional trike bikes. It has no reverse gear.

Based on the previous considerations, the design requirements for the SNAP model have been obtained to cover the largest chunk of the market:

- ease of accessibility
- full waterproofness
- comfort
- ease of battery swap
- maximum curb weight of 180 kg
- one driver seat and one passenger seat
- luggage compartment
- low maintenance and easy spare part management
- use of off-the-shelf components
- cost effectiveness around 8'000 €.

The overall goal is to fill the gap between bicycles and automobiles. Many users find it important to drive under the rain or to be able to give a ride to their children to or back from school with a bag to be placed in the trunk compartment.

Table 1 SNAP main technical specifications

Design parameter	Value
Unladen mass (kg)	130
Length (mm)	2550
Width (mm)	1250
Height (mm)	1610
Tire	24″×3″
Battery	2×980 Wh (48 V) Li-ion cells with integrated BMS (2×6 kg)
Range	approx 60 km with 2 batteries expandable up to 120 km (4 batteries)
Accessories	Front electric wiper Front electric defrost GPS tracker and 2G/3G connectivity

3 The SNAP quadricycle

The main technical specifications of SNAP are collected in Table 1, while snapshots of the proposed urban vehicle during a testing campaign are shown in Fig. 5.

Special care has been paid to the process of developing the appearance, and to some extent the ergonomics, of the vehicle. This is a laborious task since the shape of each fairing panel has been optimized to reduce the cost of the molds and the successive machining operations, while preserving at the same time a captivating look as shown in Fig. 5. The seats are adjustable, and they ensure good lateral containment in the case of impact. However, their weight is about 10 kg each. Therefore, future developments will look at the opportunity to use seats made of carbon or fiberglass with removable cover. In this case, the seat would be not reclinable, and a statistical study is required on a large user population to define the optimal size and geometry.

(a)

(b)

Fig. 5 Some views of SNAP: **a** front, **b** rear

Vehicle safety is another important aspect in the SNAP design. Anti-intrusion bars are present in both the side doors and approved safety belts are provided for both the driver and the passenger of automotive derivation with a three-point configuration. A rollbar is also present that protects passengers within the vehicle in the case of roll-over.

In the case of front impact or rear collision, reinforcements distribute the load on the chassis and deform to absorb the impact energy. Details of the anti-intrusion bars and rollbar are shown in Fig. 6 highlighted in red. The seat of automotive derivation can be appreciated as well that ensures an appropriate comfort level for the driver. E-quadricycles are heavier and are ridden at higher speed than e-bicycles. Therefore, tyres are exposed to higher stress and impact and thus need specific characteristics. SNAP adopts Vredestein's Perfect E-Power tyres that are exceptionally well-balanced. The compound is developed based on expertise developed in car tyre technology where heavy loads, stress and impact are more common. Perfect E-Power tyres are ECE-R75 certified and suitable for speeds of up to 50 km/h. They are equipped with an extra 3 mm anti-puncture layer that provides greater protection. In addition, they offer high grip in all weather conditions, even heavy rain and snow.

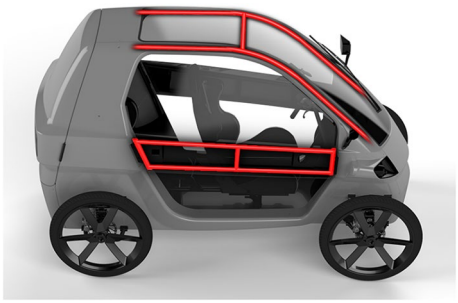

Fig. 6 SNAP safety features

As for the SNAP chassis, the design choice has been made considering both the production costs and mechanical resistance. A trade-off solution is adopted with a tubular steel chassis that allows low investment costs and relatively small weight. Future developments may certainly include the adoption of composite materials although the costs may not be fully justified. The fairings are made of ABS and they are riveted on the chassis; a solution that allows easy replacement in the case of damage.

If we refer to the Renault Twizy again, both front and rear suspension adopt a MacPherson solution. However, this suspension type requires a dedicated strut (serving at the same time as a structural and spring-damper element and participating in the steering maneuvering) that only large car manufacturers can afford and specialize for their model. Therefore, SNAP adopts a double wishbone solution with commercial spring-dampers. A tradeoff solution is pursued that limits the length of the suspension arms (about 200 mm) while ensuring a correct geometry that does not generate a large variation in the camber angle during the relative motion of tires with respect to the chassis [17].

3.1 The powertrain

The propulsion is a hybrid type achieved through pedals, operated by a single passenger, and through the assistance of an electric motor. The steering and braking of the vehicle are entrusted to the same passenger who provides the traction. The motors used on pedal assisted vehicles can be of two types: mid-drive type or in-wheel. During the vehicle design phase, both solutions were taken into consideration, i.e., a central drive motor and an external rotor motor (gearless type) which, unlike what happens on e-bikes, has not been considered installed directly in the wheel's hub.

Hereafter, for simplicity, the configuration with external rotor motor will be referred to as the "Gearless" configuration, while the central drive configuration, as the "Mid-drive". In the Gearless case (Fig. 7), the motion is

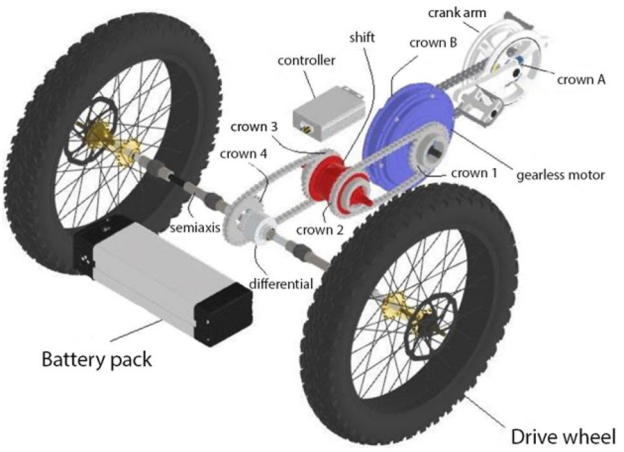

Fig. 7 Gearless type powertrain

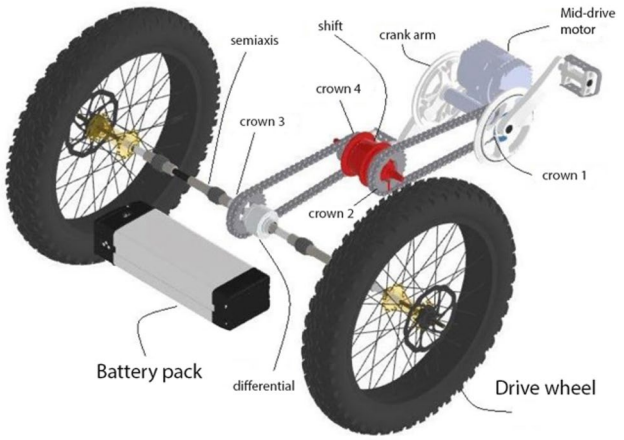

Fig. 8 Mid-drive type powertrain chosen for SNAP

transferred from the rotor of the electric motor to the differential through two chain transmissions: "1–2" from the motor to the gearbox (fixed-ratio "in-hub" type); and "3–4" from the output of the gearbox to the differential. It is observed that the crowns "B" and "1" are integral with the casing of the electric motor, which in turn is integral with the rotor.

In the Mid-drive configuration, shown in Fig. 8, we have a transmission with one less chain. The motion is transmitted by the permanent magnet brushless motor to the sprocket "1" through a reducer (ordinary), which in this case coincides with the sprocket of the crank arm, and subsequently to the wheels, by means of the same chain transmissions seen above. A gearbox with 11 gear ratios of ebike derivation transforms the power parameters in input to the rear open differential (the commercial model available for trike is used). Unlike the Gearless configuration, with the central drive motor the controller is generally installed inside the engine block and is characterized by modest dimensions. Furthermore, it can be observed that the dimensions of an external rotor motor are greater than a Mid-drive motor with the same power. In purely pedal traction, the energy is transmitted to the wheels through the two transmissions with chain "1–2", "3–4" and the fixed-ratio gearbox, but since the gearbox is integral with the crown "1", this will rotate when the motor rotates.

Table 2 Main technical specifications of SNAP Mid-drive transmission

Component	Model	Manufacturer	Part Number
Motor	250 W	Bafang	BBS
Gearbox	Alfine 11	Shimano	SG-S7001
Differential	Open diff	Samagaga	DG72N
Battery packs	Hailong 48 V Li-Ion	LG cells, 20A BMS module integrated	INR21700-M50TL

In the end, the choice fell on the Mid-drive configuration, which offers some advantages. First, it allows one to eliminate a chain, which means a clear simplification of the tensioning system of the "cascade" of chains. The Mid-drive configuration allows one to have the motor in the front area of the vehicle, both to better redistribute the weights between the front and rear axles, and to allow for a minimum footprint in the area below the seat (s) and to the load compartment. In fact, the Gearless engine has a much larger diametrical size than the other elements of the drivetrain and would have forced to sacrifice part of the internal volume of the vehicle, and to raise the center of gravity of the vehicle itself, having to move the load compartment to a higher position. Technical details of the components of the adopted Mid-drive transmission system are collected in Table 2.

3.2 Powertrain efficiency

The overall efficiency of the SNAP Mid-drive driveline can be obtained by considering the energy consumption of each component along the transmission line from the battery and the power unit to the first chain transmission, the shift, and the second chain transmission, as detailed in the remainder of this section.

3.2.1 Power supply

SNAP adopts two lithium-ion batteries of 48 V and a capacity of 980 Wh (~ 20.4 Ah), which among its

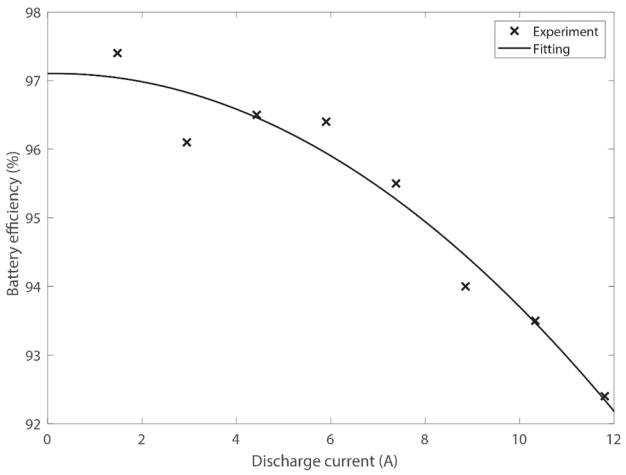

Fig. 9 Battery efficiency as a function of the discharge current

strengths is that it is very light [18]. Battery efficiency can be obtained by estimating the ratio of the output energy to the input energy, being the final and initial conditions (state of charge and temperature) the same

$$\eta_b = \frac{E_{discharge}}{E_{charge}} \quad (1)$$

Measurements of voltage (V (V)), current (I (A)), and time (t (s)) are used to calculate power P (W) and electrical energy E (J), being $P = V \times I$ and $E = P \times t$. An experimental campaign is performed to evaluate the battery efficiency as a function of the discharge current. For this purpose, the energy delivered by the battery operating at different discharge current is measured and compared with the energy stored in the battery during the charging stage. This experiment is divided into two processes: charging and discharging. For the discharge process, the electrical energy delivered by the battery was quantified by implementing a circuit in which the battery was connected to a variable resistive load and complementing the circuit with voltage and current sensors. Results are shown in Fig. 9 where experimental measurements are marked by black crosses whereas the corresponding second-order polynomial fitting ($p_0 = 97.10$, $p_1 = 0.01$, $p_2 = -0.03$) is denoted by a solid black line.

3.2.2 Power unit

The PU comprises the controller, the brushless DC motor and the reducer. The system is completed by two sensors: a Hall effect sensor and a pedal assist system (PAS) sensor. Through the measurement of the angular speed of the pedals provided by the sensor and Hall effect, an impulse is generated which is sent to the electronic control unit,

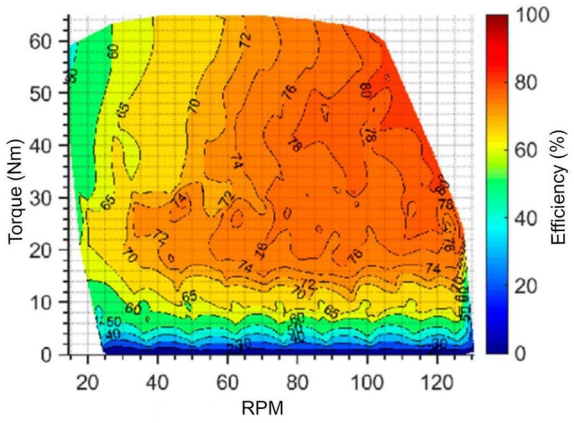

Fig. 10 Efficiency map of the power unit

which determines the starting of the engine. When started, the PAS allows the so-called "symbolic pedaling", that is, it is sufficient to turn the pedals without getting tired at all to be completely transported by the motor. The PU efficiency map expressed in terms of delivered torque and angular velocity is shown in Fig. 10, as obtained experimentally in [19]. As one can note, minimum and maximum efficiency results, respectively, in 64% and 82%.

3.2.3 Double chain transmission

The power flows from the PU to the rear tires through a double chain and an intermediate 11 speed gearbox, according to the explanatory scheme of Fig. 11.

While the performance of the shift has been previously evaluated [20], indicating an efficiency that ranges from 94% (1st gear) to 87% (11th gear), the energy consumption of the whole transmission subunit has been measured using an experimental set-up.

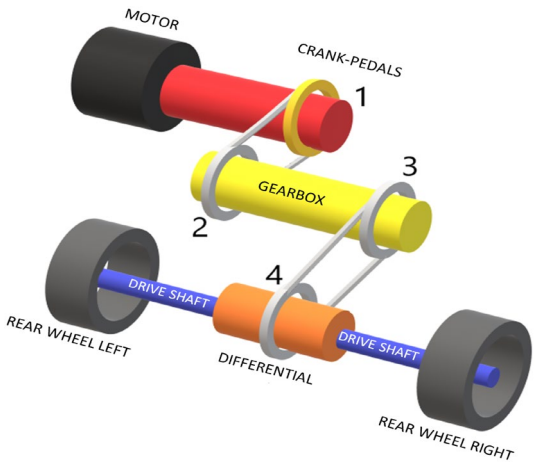

Fig.11 Scheme of the power transmission from the PU to the rear wheels

Fig. 12 Experimental set-up to estimate the double-chain transmission efficiency using a torque meter

The rear wheels of the vehicle have been lifted using two stands and a torque meter has been applied to the front hub where the pedals are mounted, making it rotate at a constant speed ω of about 2 rps ($\omega_{s,1} = 12.5$ rad/s) and reading the corresponding measured torque (Fig. 12).

Tests were carried out by varying the internal gear ratios, examining the 1st, 3rd, 5th and 7th ratio. Starting from these measurements, the efficiency of the subsystem has been evaluated following the approach proposed in [21]. The tension of the first chain $T_{c,1}$ can be determined, assuming that the tension in the lower branch was null, as the ratio between the measured torque and the radius of the crown attached with the crankshaft:

$$T_{c,1} = \frac{C_{motor}}{R_{crown}} \tag{2}$$

where the radius of the crown is calculated knowing the pitch $p = 12.7 \times 10^{-3}$ m and the number of teeth $N_{s,1} = 44$:

$$R_{crown} = \frac{p \cdot N_{s,1}}{2\pi} \tag{3}$$

while the rotation speed of the driven sprocket can be estimated using the transmission ratio relative to the first chain (τ_1):

$$\omega_{s,2} = \tau_1 \cdot \omega_{s,1} \tag{4}$$

Then, it is possible to obtain the energy loss due to the lateral displacement between the bush and the pin (W_{pin}) and the energy loss between the bush and the roller in the stretch of branch in tension of the chain (W_{bush}). To evaluate these two entities, the following parameters have been used [21]:

- $\mu_1, \mu_2 = 0.11$, friction coefficient between the bush and the roller
- $R_{bi} = 1.74\ 10^{-3}$ m, inner radius of the bush
- $R_{bo} = 2.83\ 10^{-3}$ m, outer radius of the bush
- $\gamma = 0$, lateral offset angle
- $\theta = \frac{360}{N_s} \cdot \frac{\pi}{180}$ rad, angle between the axis of the chain branch and the seated link in the sprocket
- $\beta = 40°$, nominal pressure angle

Then:

$$W_{pin,1} = \frac{\pi}{2} \cdot \left(\frac{1}{\sqrt{1+\mu_1{}^2}} \cdot T_{c,1}\right) \cdot \mu_1 \cdot R_{bi} \cdot \theta \tag{5}$$

and

$$W_{bush,1} = \frac{\pi}{2} \cdot \frac{sin\theta}{\sqrt{1+\mu_2{}^2} \cdot sin(\beta - \theta)} \cdot T_{c,1} \cdot cos\gamma \cdot \mu_2 \cdot R_{bo} \cdot \theta \tag{6}$$

Losses due to damping have been neglected compared to the previous friction components considering that the two chains are made out of steel. It is therefore possible to calculate the efficiency of the first chain η_1 and the torque acting on the intermediate pinion that precedes the shift as:

$$\eta_1 = \frac{C_{p1} \cdot \omega_{s,2}}{C_{p1} \cdot \omega_{s,2} + N_{s,1} \cdot \omega_{s,1} \cdot \left(W_{pin} + W_{bush}\right)} \tag{7}$$

$$C_{p1} = \frac{\eta_1 \cdot C_{\text{motor}}}{\tau_1} \tag{8}$$

After analyzing the first chain, we can move on to the second one considering the presence of the gearbox. In fact, the torque acting on the toothed wheel following the gearbox (C_{p2}) is given by the ratio between the torque acting on the pinion prior to the gearbox and the transmission ratio:

$$C_{p2} = \frac{\eta_{gearbox} \cdot C_{p1}}{\tau_{gearbox}} \tag{9}$$

The angular speed of the pinion at the gearbox output, which acts as the driving wheel of the second chain can be obtained as:

$$\omega_{p2} = \omega_{p1} \cdot \tau_{gearbox} \tag{10}$$

Similarly, it is possible to arrive at the efficiency of the second chain that connects the internal gearbox with the differential:

$$\eta_2 = \frac{C_{p3} \cdot \omega_{s,3}}{C_{p3} \cdot \omega_{s,3} + N_{s,2} \cdot \omega_{s,2} \cdot \left(W_{pin,2} + W_{bush,2}\right)} \tag{11}$$

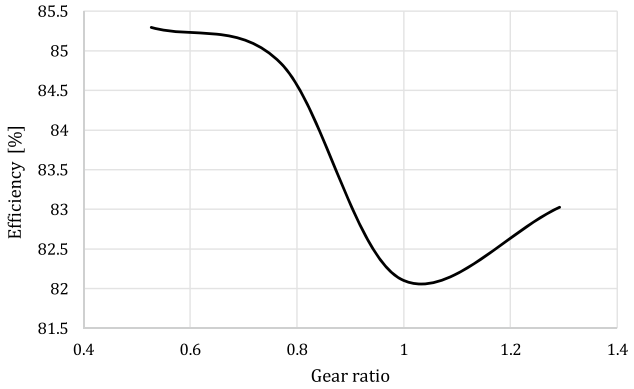

Fig. 13 Efficiency of the transmission composed by the double chain and the internal shift as a function of the gear ratio

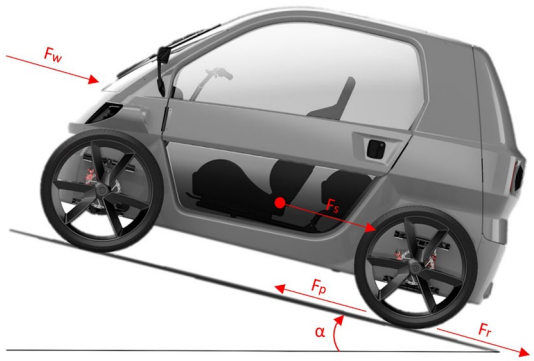

Fig. 14 Longitudinal dynamics for SNAP

where in this case with the subscript 3, it is indicated the quantities referred to the driven wheel of the second chain. Once the efficiency of the two chains has been obtained, it is possible to obtain the overall transmission performance given by the two chains and the internal gearbox:

$$\eta_{tot} = \eta_1 \cdot \eta_2 \cdot \eta_{gearbox} \tag{12}$$

The entire procedure has been repeated for different torques on the crankshaft, as the ratio was changed. The results are shown in Fig. 13. It can be noted that the efficiency of the chains is not particularly influenced by the gear ratio. An efficiency of over 95% is obtained for both chains, with the efficiency of the overall system consisting of the two chains and the internal gearbox, which is influenced by that of the 11 speed gearbox and it is included in the 83–85% range.

3.3 SNAP efficiency

Consider SNAP shown in Fig. 14. A simple model for the longitudinal dynamics is

$$F_p - \left(F_r + F_S + F_W\right) = Ma_x \tag{13}$$

where M includes the prototype vehicle mass (185 kg) and that of one driver (75 kg).

- F_p is the tractive effort developed by the rear axis
- F_r is the rolling motion resistance, $F_R = M \cdot g \cdot C_r \cdot cos\alpha$, with g the gravity acceleration, C_r the coefficient of rolling resistance (= 0.01), and α the road slope
- F_S is the motion resistance due to gravity, $F_S = M \cdot g \cdot sin\alpha$
- F_W is the aerodynamic resistance, $F_W = \frac{1}{2} C_d \cdot \rho \cdot A \cdot v^2$, with ρ the air density (= 1.2 kg/m^3), C_d the aerodynamic resistance (= 0.64), A the front area of the vehicle (= 1.32 m^2), and v the longitudinal velocity.

Under the assumptions of steady-state condition, flat road and no effort applied by the driver, Eq. (13) can be used to get the tractive effort given a certain velocity and gear. Then, the corresponding operating point in terms of torque and angular velocity of the drive shaft can be obtained on the PU map as:

$$T_{crankspindle} = \frac{F_P \cdot r_w \cdot \tau_1 \cdot \tau_{gearbox} \cdot \tau_2}{\eta_{tot}}$$

$$RPM_{crankspindle} = \frac{RPM_w}{\tau_1 \cdot \tau_{gearbox} \cdot \tau_2}$$

being r_w the tire rolling radius (= 0.3 m), and $RPM_w = v \cdot \frac{60}{2\pi \cdot r_w}$ the tire angular velocity. Two types of curves can be considered:

- iso-gear curve that collects the possible operating conditions for varying travel speed while keeping the same gear ratio (denoted in black).
- iso-speed (or iso-power) curve that describes the possible operating conditions of the PU at the same travel speed while varying the gear ratio (marked in red).

In Fig. 15, iso-gear and is-speed curves are overlaid over the PU efficiency map. The energy consumption is generally lower for high gear ratio and speed, whereas it drops dramatically in the case of low velocity. The first-gear drive shows the lowest efficiency especially during slow drive (e.g., lower than 1.5 m/s or 47 rpm) where it approaches just over 50%. For high speeds there is an increase in efficiency for each gear ratio in the internal gearbox, reaching

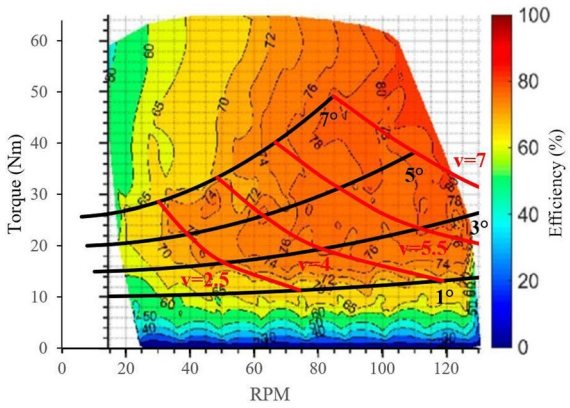

Fig. 15 PU efficiency map with overlaid iso-speed (red) and iso-gear curves (black). Steady-state drive on a flat road

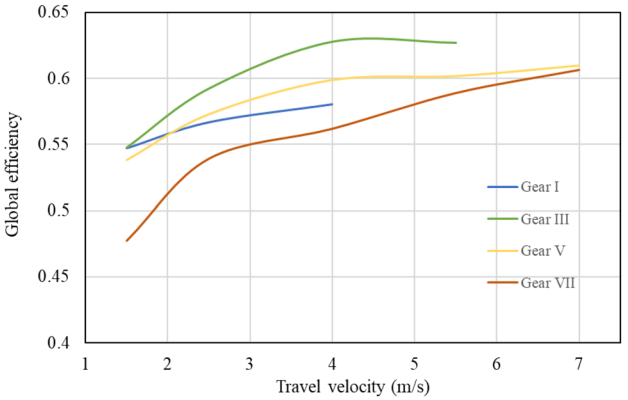

Fig. 17 Global efficiency as a function of the travel speed at constant gear ratio. Steady-state drive on a flat road

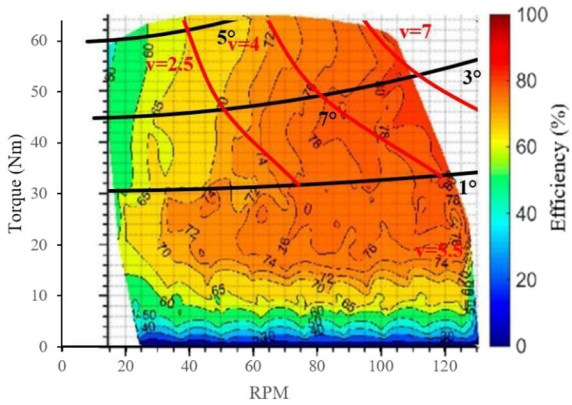

Fig. 16 PU efficiency map with overlaid iso-speed (red) and iso-gear curves (black). Steady-state drive on a 2% sloped road

the highest efficiency in the third gear, where an average efficiency of 78–79% is noted. It is interesting to see what happens when driving uphill. The corresponding iso-gear and iso-speed curves for a 2% slope are overlaid on the motor map in Fig. 16. As one would expect, for higher gear ratios the iso-gear curves exceed the efficiency map. The maximum efficiency of about 80% is reached for the first and third gear when speeds exceed 3 m/s (e.g., 70 rpm). The lower the speed, the worse the efficiency.

The overall vehicle efficiency that includes battery, PU, and chain transmission, can be expressed as a function of the travel speed for the case of zero slope and constant gear ratio, as shown in Fig. 17. The third-gear and seventh-gear drive ensure, respectively, the best and worst performance.

The distribution of the energy loss between the different elements of the SNAP transmission is shown in Fig. 18. At lower speeds the largest loss is that of the power unit, while increasing the speed, the contributions of the transmission (two chains and gearbox) and that of the battery have a larger impact. However, the main source of dissipation remains the power unit.

Finally, when considering the energy consumption per traveled distance (Wh/km) as a function of the vehicle speed and gear, it is confirmed that the lower the speed the higher the efficiency and that the third-gear drive provides the best performance, as shown in Fig. 19.

Experimental tests have also been performed on a circuit to validate the previous energy assessment and state the vehicle's mileage values. These tests have been carried out with the vehicle in a 250 W configuration and a single 980 Wh battery. The reduced weight of each battery pack equal to 6 kg, in fact, does not significantly affect the test results, as the weight of the secondary battery pack not installed, caused a weight variation of the vehicle of less than 3%. In this way, by installing a single battery, it has been possible to obtain results by performing more tests with half the mileage. In all the tests, an alpha prototype of SNAP was adopted, which had a weight of 185 kg, rather than the 130 kg of the final product. It covered 22.02 km against the 30 km that theoretically it should have traveled. However, considering the considerably larger weight of the prototype, due to the production technique of the bodywork, which was made in 3D printing and then laminated in fiberglass, the result can be considered as fully within the theoretical predictions.

3.4 Maximum speed

In this section, the performance of SNAP in terms of gradeability and maximum speed is investigated. The longitudinal dynamics model of Eq. (13) can be formulated as follows

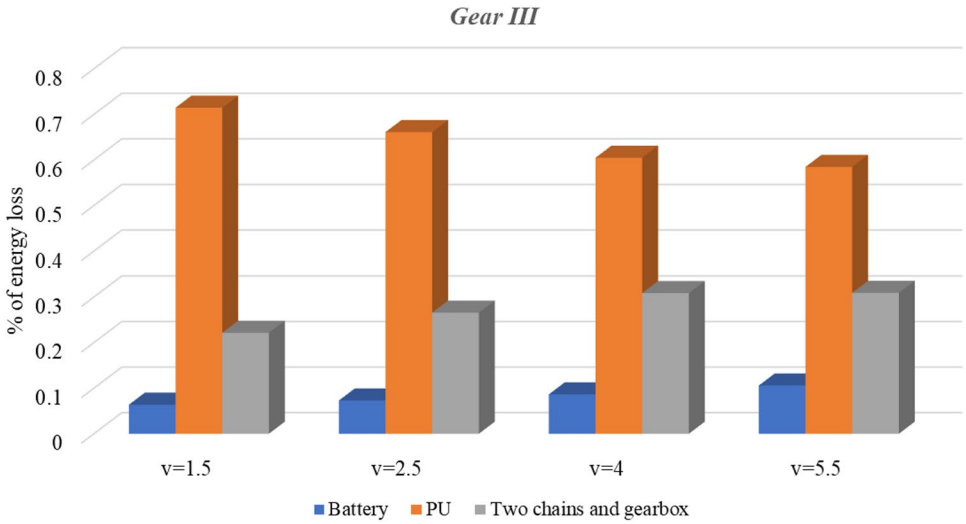

Fig. 18 Distribution of energy loss in the transmission components as a function of travel speed (m/s)

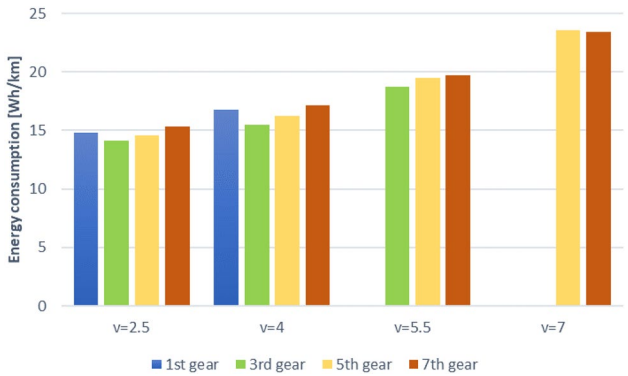

Fig. 19 Energy consumption per traveled distance as a function of travel velocity and gear

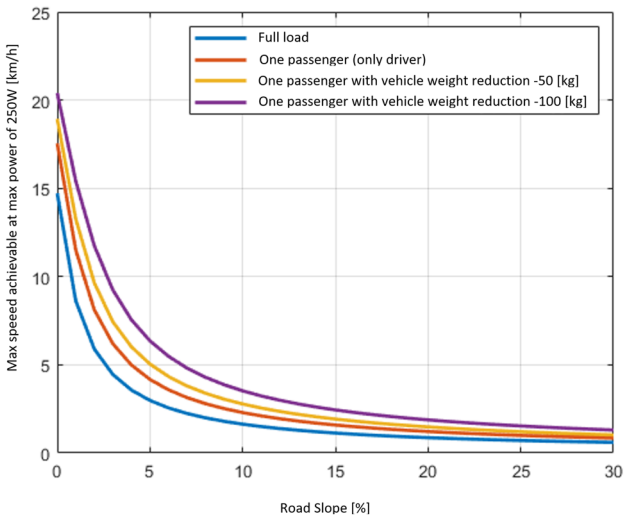

Fig. 20 Maximum achievable speed as a function of road slop

$$P_{max}n_{tot} = \left(Mgsin\alpha + Mgcos\alpha f + \frac{1}{2}\rho C_x A V_{max}^2\right)V_{max} \quad (14)$$

where the lowest power configuration (P_{max}= 250 W) is considered, V_{max} is the maximum speed, and η_{tot} is the efficiency of the entire transmission. The maximum achievable speed can be estimated varying the road slope as shown in Fig. 20. In the case of flat road, and with one driver only, the maximum velocity results in 17.5 km/h reducing to 14.7 km/h in the case of full payload consisting of a 190 kg payload (two 75 kg passengers + 40 kg luggage).

As expected, increasing the road slope results in a reduction in the maximum achievable speed. At the highest road slope of 30%, the maximum speed results in 1.5 and 1 km/h, respectively for the one driver and full load condition.

4 Discussion

This paper deals with the new concept of SNAP, a pedal-assisted four-wheel cargo bike that aims to fill the gap between e-bicycle and e-car. Relevant aspects to evaluate the performance of such a vehicle in terms of maximum speed, efficiency, and travel range at varying operating conditions have been addressed in a timely manner. Previous research in this field has been very limited. There are no scientific articles specifically related to electric pedal-assisted vehicles, and of the little material available in the literature, including [22–26], none addresses the performance aspect. The physics and performance of the bicycles in a planar and sloped motion have been presented in [22] and laid the foundations to extend the study to cargo and pedal assisted

vehicles with the additional power constraint of 250 W. This regulatory power limit has made the design of SNAP very difficult, as the overall weight must be kept very low. Special attention has been devoted to assessing the vehicle performance and understanding if it is possible to use it in urban settings and what are its limits of use.

It was found that the highest efficiency (about 60%) can be reached at medium/high travel velocities (greater than 15 km/h) in low/medium gear. Low travel velocities are generally characterized by high energy consumption. It is also interesting to note that the higher the travel velocity the larger the energy loss in the double chain transmission that can reach up to 30% of the total energy dissipation of the powertrain. This is an aspect open to improvement for future developments. The drive motor efficiency map shows great variability with the operating conditions. Low speed and high torque ranges should be especially avoided, indicating another critical point related with the requirement of a correct choice of the coupling of the drive motor with an appropriate reducer. In the case of flat road, and with one driver only, the maximum velocity resulted in 17.5 km/h that, however, reduces to 14.7 km/h in the case of full payload. The overall characteristics of SNAP also make it very competitive compared to market competitors, both from a technical point of view, just remember the aspects of safety, comfort, design and protection from atmospheric agents, but also from the point of view of price, which turns out to be very competitive with an actual cost of about 8'000 € and an estimated base selling price starting from 10'000 €, which is lower than the existing market competitors.

5 Conclusions

The paper presented a new concept in sustainable mobility. SNAP is a four-wheel pedal-assisted electric vehicle that meets modern sustainability requirements. The proposed urban vehicle features limited size and weight to increase efficiency and dexterity in the narrow city streets, increased safety and comfort for the driver and possible passenger, and payload capacity to fulfill last mile delivery applications. The whole design was aimed towards low maintenance and complexity. As a result, some components may appear oversized with respect to the load conditions expected for this type of vehicle. For example, the suspension arms could have been made out of composite materials, ensuring lower weight but making repairments very expensive. In the case of SNAP, the choice of steel allows repairing with a standard continuous wire welding machine to restore both the chassis and the suspensions.

Future developments will investigate the adoption of new materials as well as the adoption of novel drivetrain architectures that avoid the use of chains for power transmission or adopt multiple small electric motors [27]. The integration of driving assistance systems will be also investigated to monitor safety parameters [28].

Acknowledgements Preliminary parts of this paper were presented at 1st Workshop IFToMM for Sustainable Development Goals (I4SDG), held online on November 25-26, 2021.

Author contributions All authors contributed equally to the study conception and design of the research. All authors read and approved the final manuscript.

Funding Vincitore PIN/Winner of PIN – Iniziativa promossa dalle Politiche Giovanili della Regione Puglia e ARTI e finanziata con risorse del FSE – PO Puglia 2014/2020 Azione 8.4 e del Fondo per lo Sviluppo e la Coesione—Initiative promoted by the Youth Policies of the Puglia Region and ARTI and funded with resources from the ESF—OP Apulia 2014/2020, Action 8.4 and the Development and Cohesion Fund. The financial support of the projects: Agricultural inTeroperabiLity andAnalysis System (ATLAS), H2020 (Grant No. 857125), and multimodalsensing for individual plANT phenOtyping in agriculture robotics (ANTONIO), ICTAGRI- FOOD COFUND (Grant No. 41946) is gratefully acknowledged.

Data availability The datasets generated during and/or analysed during the current study are available from the corresponding author on reasonable request.

Declarations

Conflict of interest On behalf of all authors, the corresponding author states that there is no conflict of interest. G. Reina and G. Mantriota declare they have no financial interests to disclose. F. Passarella is the CEO of the innovative start-up SNAP and pursuing his research doctorate in urban micro-mobility at the Polytechnic University of Bari.

Ethical approval The authors declare that there is no ethical issue applied to this article.

Consent to participate The authors agree with the participation.

Consent to publication The authors declare that all authors agree to sign the transfer of copyright for the publisher to publish this article upon on acceptance.

References

1. Eric Melin H (2019) Analysis of the climate impact of lithium-ion batteries and how to measure it. Circular Energy Storage. Commissioned by Transport & Environment
2. Sticchi Damiani A (2021) La transizione energetica della mobilita' deve essere sostenibile (Italian). In: 75th Italian conference of traffic and circulation, Rome
3. Gartner J, Citron R (2016) Electric bicycles Li-ion and SLA E-bikes: drivetrain, motor, and battery technology trends, competitive landscape, and global Market forecasts, Boulder, USA, 15 June 2016
4. Braune S, Kramer K, Meissner K (2013) Electric drive system for a vehicle driven by muscle power. DE Patent 201,310,012,208, 17 July 2013
5. Sveje N, Hansan J, Nielsen O (2017) An electric vehicle with controllable generator. EP Patent 3,110,687, 01 Apr 2017
6. Son H, Kawn S (2014) Electric bicycle driving apparatus. EP Patent 2,711,239, 26 Mar 2014
7. "About," PODBIKE. https://www.podbike.com/about/. Accessed 19 Apr 2018
8. "HYBRID POWER," Hybrid Power. http://www.twike.com/en GB/vehicles/twike-3/hybrid-power/. Accessed 19 Apr 2018
9. Kronfeld R, Smith L, Bockin R, Castellotti S (2013) Human-rechargeable electric vehicle. US Patent 20,130,081,892 A1, 04 Apr 2013
10. EN 15194:2017. Cycles—electrically power assisted cycles—EPAC Bicycles, Standards
11. Passarella F, Mantriota G, Reina G (2021) The SNAP: a novel four-wheel pedal-assisted electric lightweight vehicle. Proceedings of I4SDG workshop 2021. I4SDG 2021. Mechanisms and machine science, vol 108. Springer, Cham. https://doi.org/10.1007/978-3-030-87383-7_12
12. https://www.velomobiles.co.uk/tag/bluevelo/. Accessed 15 May 2021
13. Ti-FLY X Homepage. https://azub.eu/recumbent-bikes-and-trikes/trikes/26-wheels/ti-fly-x/. . Accessed 15 May 2021
14. EAV Homepage. https://eav.solutions/. Accessed 11 Dec 2022
15. CITKAR Homepage. https://citkar.com/en/. Accessed 11 Dec 2022
16. VELOVE Homepage. https://www.velove.se/. Accessed 11 Dec 2022
17. Reina G, Foglia M (2013) On the mobility of all-terrain rovers. Ind Robot 40(2):121–131
18. Hung NB, Lim O (2020) A review of history, development, design and research of electric bicycles. Appl Energy 260:114323
19. Arango I, Lopez C, Ceren A (2021) Improving the Autonomy of a Mid-Drive Motor Electric Bicycle Based on System Efficiency Maps and Its Performance. World Electr Veh J 12:59
20. https://bikeshed.johnhoogstrate.nl/bicycle/drivetrain/shimano_alfine_inter_11/
21. Zhang S-P, Tak T-O (2020) Efficiency estimation of roller chain power transmission system. Kangwon National University, Chun Cheon, Department of Mechanical and Biomedical Engineering
22. Wilson DG (2020) Bicycling science. MIT, Cambridge
23. Vasiutina H, Szarata A, Rybicki S (2021) Evaluating the environmental impact of using cargo bikes in cities: a comprehensive review of existing approaches. Energies 14(20):6462
24. Temporelli A, Brambilla PC, Brivio E, Girardi P (2022) Last mile logistics life cycle assessment: a comparative analysis from diesel van to e-cargo bike. Energies 15(20):7817
25. Chinubhai Shah V (2018) Master's Final Degree Project. Designing and Investigating of Electric Tricycle, Kaunas University of Technology, Mechanical Engineering and Design Faculty
26. Bakker R (2016) Mechanical design and prototyping of a four-wheeled velomobile concept. Master Thesis, University of Twente
27. Mantriota G, Reina G (2021) Dual-motor planetary transmission to improve efficiency in electric vehicles. Machines 9(3):58
28. Reina G, Gentile A, Messina A (2015) Tyre pressure monitoring using a dynamical model-based estimator. Veh Syst Dyn 53(4):568–586